



# Effects of Temperature, Molecular Weight, and Non-Solvent Variation on the Physical Properties of PVDF Membranes Prepared through Immersion Precipitation

Resa Wulandari <sup>1,2</sup>, Edi Pramono <sup>2,\*</sup>, Sun Theo Constan Lotebulo Ndruru <sup>3,\*</sup>,  
 Abu Masykur <sup>2</sup>, Sayekti Wahyuningsih <sup>2</sup>, Aditya Muhammad Fadhilah <sup>2</sup>,  
 Ellya Syaharani <sup>2</sup>, Elva Yoga Saputra <sup>2</sup>, Mayzy Vanesia Insani <sup>2</sup>

<sup>1</sup> Master Program of Chemistry, Faculty of Mathematics and Natural Sciences, Universitas Sebelas Maret, Surakarta, Indonesia

<sup>2</sup> Chemistry Department, Faculty of Mathematics and Natural Sciences, Universitas Sebelas Maret, Surakarta, Indonesia

<sup>3</sup> Research Center for Chemistry, National Research and Innovation Agency (BRIN), PUSPIPTEK Area Serpong, Tangerang Selatan, Banten, Indonesia

\* Corresponding author: [edi.pramono.uns@staff.uns.ac.id](mailto:edi.pramono.uns@staff.uns.ac.id)

<https://doi.org/10.14710/jksa.27.1.35-44>

## Article Info

### Article history:

Received: 27<sup>th</sup> October 2023

Revised: 22<sup>nd</sup> January 2024

Accepted: 06<sup>th</sup> February 2024

Online: 19<sup>th</sup> February 2024

### Keywords:

Immersion precipitation;  
 Membrane structure; PVDF

## Abstract

Research on porous membrane technology is proliferating, especially in the process of fabrication of membranes. Different methods in membrane fabrication can affect the physical and chemical properties of the produced membrane. This study aims to investigate the influence of temperature, molecular weight, and non-solvent type on the physical-chemical properties of PVDF membranes. The membrane was produced by the immersion precipitation method with varying PVDF molecular weights of 64 kDa, 352 kDa (Solef 1010), 534 kDa, and 573 kDa (Solef 1015); non-solvent variations of alcohol (methanol, ethanol, isopropyl alcohol, and butanol); and drying temperature variations of 40, 50, and 60°C. The produced membranes were analyzed using ATR-FTIR, XRD, TGA, DSC, and SEM, and their wettability properties were evaluated using water contact angles. The optimal drying temperature for membrane production was 60°C. The ATR-FTIR data showed that molecular weight impacted membrane structure, where PVDF MW 534 kDa membrane had the highest percentage of  $\beta$  phase (77.47%). Non-solvent changes also affected membrane structure; PVDF Solef 1010 with non-solvent isopropyl alcohol had the highest percentage of  $\beta$  phase (67.45%). This is supported by the XRD diffractogram that displayed peaks at  $2\theta$  values between 20.24° and 20.66°, indicating the presence of a phase  $\beta$  PVDF. The thermal analysis exhibited three stages of degradation for Solef 1010 with ethanol non-solvent and two for the other seven membranes. The degradation temperature increases with the increase in molecular weight and the difference in non-solvents. The highest thermal stability membrane was PVDF Solef 1010 with isopropyl alcohol non-solvent (430°C). SEM images showed the membrane with non-solvent isopropyl alcohol, displaying a dense sponge-like morphology. The wettability of membranes is affected by molecular weight and non-solvent type. The membrane with isopropyl alcohol non-solvent obtained the smallest contact angle (54.77°) and indicated the most wettability membrane.

## 1. Introduction

Porous membrane technology has become prevalent across many fields due to its convenient production methods using various materials and fabrication

techniques [1]. Porous membranes are frequently employed in many applications, such as water purification [2], battery separators [3], and gels or solids polymer electrolytes in batteries [4]. The basic materials for fabricating membranes can be categorized into

ceramics and polymers. The significant chemical resistance of polymeric materials, like polysulfone (PS), polyvinylidene fluoride (PVDF), and polypropylene (PP), makes them popular choices for use in the production of commercial membranes [5].

Polyvinylidene fluoride (PVDF) has high mechanical strength, good chemical resistance, good thermal stability, and exceptional resistance to membrane degradation, all of which are crucial attributes for their application in high-pressure environments [6]. Polyvinylidene fluoride (PVDF) is synthesized via free radical polymerization using vinylidene fluoride monomers, resulting in a diverse distribution of molecular weights attributed to varying polymerization rates [7]. The influence of the molecular weight of polyvinylidene fluoride (PVDF) affects several elements, such as rheological effects on polymer solutions, thermodynamic and kinetic, membrane structure, and other physical properties inside a PVDF membrane [8].

Besides molecular weight, several parameters affect the morphology and performance of the fabricated membrane, including polymer concentration in the dope solution, the strength of the non-solvent employed in the coagulant bath, the incorporation of additives, and the temperature (dope solution temperature and coagulant bath) [9]. Different fabrication methods for PVDF membranes also impact their physical properties, especially polymorphs [10]. The phase inversion approach is popular because it can produce membranes in controlled ways, with simple processing and low-cost production [1, 11].

In the immersion precipitation method, solvent and non-solvent are exchanged to form a membrane. In the polymer melting process in the immersion precipitation method, melting using a solvent with a temperature of  $< 70^{\circ}\text{C}$ , a  $\beta$  phase will be formed, as long as the solvent used is a good solvent for PVDF [12]. It is important to pay attention to the temperature when preparing membranes. Whether it is the temperature of the dope solution, the temperature of the coagulant bath, or the casting device because the temperature plays a significant role in influencing the kinetics of membrane formation and the resulting membrane's morphology [13, 14].

Selecting non-solvents in this method also plays a crucial role in influencing the precipitation of the membrane. When a dope solution is cast on a petri dish and subsequently immersed in a non-solvent, the miscibility of solvent and non-solvent, along with the affinity between the polymer and non-solvent, determines the exchange rate and the ultimate structure of the membrane. Utilizing "soft" non-solvent-like alcohol leads to a precipitation process that yields a particulate morphology [9, 13].

Several studies have investigated the effect of various molecular weights of PVDF [10, 15, 16, 17]. Haponska *et al.* [10] reported an immersion precipitation method using NMP as solvent and water as non-solvent with different temperatures of non-solvents at 20, 40, and  $60^{\circ}\text{C}$ . The result showed that the membrane produced at  $20^{\circ}\text{C}$  has a reasonably high  $\beta$  phase and dense structure. Chang *et al.*

[9] investigated the impact of non-solvents in the form of propanol, isopropanol, butanol, and 1-octanol on PVDF with MW 254 kDa, resulting in membranes that had only  $\alpha$  and  $\gamma$  type polymorphs for all membranes using non-solvents propanol, isopropyl alcohol, butanol, and 1-octanol. Also, it produced membrane morphology with a globular shape.

Meanwhile, comprehensive information and research on the effect of temperature, coagulant type, and molecular weight on the physical properties of PVDF membranes through immersion precipitation methods is still limited. This study investigates the effect of molecular weight variations on four different PVDF polymers and the influence of non-solvent alcohols on PVDF with a molecular weight of 352 kDa. The investigation aims to determine the effects on various physical properties of the membranes, including the types of polymorphs formed, crystallinity, thermal degradation, melting point, and wettability.

## 2. Experimental

### 2.1. Materials

Polyvinylidene fluoride (PVDF) Solef 1010 (MW: 352 kDa) and PVDF Solef 1015 (MW: 573 kDa) were obtained from Solvay. PVDF (MW: 64 kDa) was obtained from Jiangsu Freechem-China, and PVDF (MW 534 kDa) was obtained from Sigma Aldrich. N'-N-Dimethylacetamide (DMAc), methanol, ethanol, isopropyl alcohol (IPA), and butanol were purchased from Merck.

### 2.2. Fabrication of PVDF Membranes

PVDF membranes were produced by dissolving each 18% (wt%) PVDF (PVDF with MW of 64 kDa, 352 kDa (Solef® 1010), 534 kDa, and 573 kDa (Solef® 1015)) into 82 wt% DMAc. This solution was homogenized for 24 hours at  $60^{\circ}\text{C}$  to produce a dope. The dope was cast on a glass plate and immersed in ethanol as a non-solvent. The resulting flat membrane was dried in an oven at  $60^{\circ}\text{C}$  for one hour. To introduce variations in the non-solvent, methanol, ethanol, isopropyl alcohol, and butanol were used. Additionally, PVDF membranes were dried in an oven at temperatures of 40, 50, and  $60^{\circ}\text{C}$  to investigate the impact of drying temperature.

### 2.3. Characterization

The membranes were subsequently characterized using ATR-FTIR, XRD, Water Contact Angle (WCA), SEM, TGA, and DSC. The functional groups of the membrane were analyzed using ATR-FTIR. The  $\beta$  phase was determined using Equation (1).

$$F(\beta) = \frac{A_{\beta}}{(K_{\beta}/K_{\alpha})A_{\alpha} + A_{\beta}} \quad (1)$$

Where  $F(\beta)$  represents the  $\beta$ -phase content,  $A_{\alpha}$  and  $A_{\beta}$  denote the absorbance at  $763$  and  $833\text{ cm}^{-1}$ ,  $K_{\alpha}$  and  $K_{\beta}$  are the absorption coefficients at the respective wavenumber, with values of  $6.1 \times 10^4$  and  $7.7 \times 10^4\text{ cm}^2\text{mol}^{-1}$ , respectively.

The crystallinity data and crystal structure changes of the produced PVDF membrane were determined using XRD. The obtained information consisted of the intensity

of the peaks that appear at the specified diffraction angle. Then, the degree of crystallinity was calculated using Equation (2).

$$\text{Degree of crystallinity} = \frac{A_c}{(A_a + A_c)} \times 100\% \quad (2)$$

Where  $A_c$  represents the total area of the crystalline phase, and  $A_a$  represents the total area of the amorphous phase.

WCA measurement was conducted to determine the wettability of the PVDF membrane by dripping water on the membrane surface. The images were then captured with a super-macro camera and analyzed using ImageJ software. The membrane morphology was assessed by examining the membrane cross-section using Scanning Electron Microscopy (SEM). Additionally, Thermogravimetric Analysis (TGA) and Differential Scanning Calorimetry (DSC) were employed to assess the thermal stability and melting temperature of the PVDF membranes.

### 3. Results and Discussion

#### 3.1. Fabrication of PVDF Membranes with Drying Temperature Variations

Using different non-solvents causes differences in the time of membrane precipitation and the physical appearance of each membrane. Figure 1 shows the results of membrane fabrication at 40, 50, and 60°C. For methanol, ethanol, and isopropyl alcohol, membrane formation at a drying temperature of 40°C requires 2 hours, whereas butanol necessitates more than 3 hours for membrane formation. This trend persists at 50°C and 60°C, where methanol, ethanol, and isopropyl alcohol exhibit faster membrane formation than butanol.

The observed differences in membrane formation times can be attributed to the unique mixing characteristics of solvents and non-solvents in the membrane formation system. Non-solvents that exhibit poor mixing with solvents tend to result in delayed membrane development [13]. The delayed time in membrane formation can be used to determine the precipitation rate. The longer the time required for membrane formation, the slower the precipitation rate. The exchange rate of non-solvent and solvent can explain the difference in precipitation rate (determination of diffusion coefficient ( $D^0$ ) of non-solvent with solvent) [18].

**Table 1.** Delay time and diffusion coefficient between non-solvent and DMAc [18]

Non solvent	Delay time (s)	$D^0_{\text{non-solvent-DMAc}} \times 10^{-6}$ (cm <sup>2</sup> /s)
Water	0	24.61
Methanol	6.6	20.63
Ethanol	10.2	17.64
Isopropyl alcohol	16.3	15.75

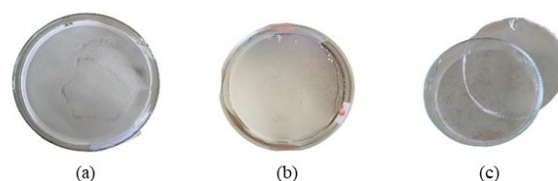


**Figure 1.** PVDF membranes dried in an oven at a) 40°C, b) 50°C, and c) 60°C

Table 1 presents the values of the distribution coefficients of several alcohols against DMAc. The delay time in membrane formation increases as non-solvent  $D^0$  from methanol, ethanol, and isopropyl alcohol decreases. Furthermore, in the use of solvents from DMAc, Dimethylformamide (DMF), and N-methylpyrrolidone (NMP),  $D^0$  decreased with non-solvent variations in the order of methanol > ethanol > isopropyl alcohol > butanol, with butanol having the longest delay time among all the non-solvents employed [19, 20]. Thus, the observed trend is consistent with the outcomes of the conducted experiments.

The membrane obtained at 40°C (Figure 1a) is extremely dry and impossible to use, whereas the membrane obtained at 50°C (Figure 1b) has a physical shape similar to a gel and a transparent appearance. However, this gel-like nature causes membrane damage upon removal from the petri dish, indicating that its mechanical properties may not be suitable for certain applications. In contrast to the membranes produced at 60°C (Figure 1c), this membrane is a non-brittle nature and is easily detached from a petri dish, allowing it to be utilized in various applications.

A temperature of 60°C has been commonly employed in similar methods for both PVDF and other polymers, as demonstrated by several other studies, including those conducted by Hussain *et al.* [21] and Ashtiani *et al.* [22]. In this research, PVDF membranes were dried in an oven at a temperature of 60°C for 60 minutes for non-solvents such as methanol, ethanol, and isopropyl alcohol. For the non-solvent butanol, the drying time was extended to 75 minutes.

#### 3.2. PVDF Membranes with Various Molecular Weight

Figure 2 shows ATR-FTIR spectra of PVDF membranes based on polymers with molecular weights of 352 kDa (Solef 1010) and 573 kDa (Solef 1015) and PVDF with molecular weights of 64 and 534 kDa in ethanol non-solvent. Among the four membranes, there is an absorption of  $\alpha$  phase whose absorbance intensity is relatively high in PVDF Solef 1010 and PVDF Solef 1015 at wavenumbers 763, 795, 975, 1203, and 1383 cm<sup>-1</sup> [11, 23, 24, 25]. The appearance of absorption at wavenumber around 1070 and 1170 cm<sup>-1</sup> indicate the presence of the  $\beta$  phase, while 833 cm<sup>-1</sup> is a shift from the absorption  $\beta$  phase [12, 26, 27]. This is supported by XRD data (Figure 3), with the occurrence of the peaks at  $2\theta = 20.2$ – $20.6^\circ$  as the main peak of the  $\beta$  phase [12, 27].

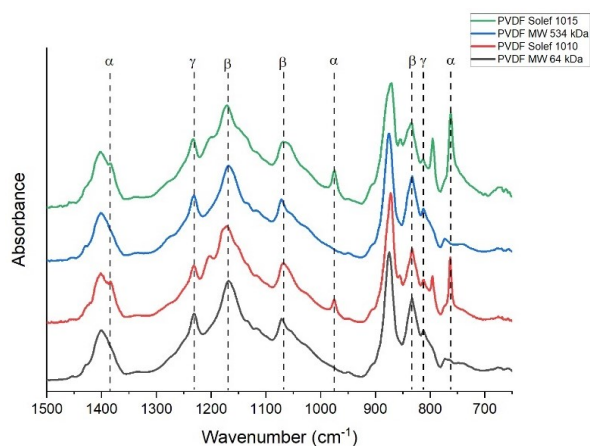


**Figure 2.** ATR-FTIR spectra of PVDF membranes with different molecular weights

High intensity at  $2\theta = 21.3^\circ$  and  $23.6^\circ$  are related to polyethylene-like structure [28], which indicates the presence of the  $\beta$  phase because the structure of polyethylene is similar to the  $\beta$  phase of PVDF. In addition, the XRD diffractogram shows intensities at  $2\theta = 17.95^\circ$ ,  $26.7^\circ$ , and  $38.8^\circ$ , which indicates the  $\alpha$  phase [12, 26]. The crystallinity of the membrane can also be measured from XRD data. The lowest crystallinity was obtained in Solef 1010 with  $\beta$  phase 49.69%. The crystallinity data and the  $\beta$  phase content of the produced membrane can be seen in Table 2.

The formation of  $\beta$  phase corresponds to the dipole moment of the solvent. When solvents with high dipole moments interact with PVDF, the  $\beta$  phase is easily formed [23]. Thus, it can be said that hydrogen bonding in PVDF and solvent is the crucial factor governing the formation of the  $\beta$ -phase. An interface hydrogen bond is formed between the hydrogen or fluorine atoms in the PVDF and the solvent [23]. In addition, according to the rule of “Polar Soluble in Polar,” the interaction between DMAc and  $\beta$ -PVDF solvents is strong. Hence, it can form a  $\beta$  phase in PVDF membranes [24]. In addition,  $\beta$ -PVDF phase formation depends on delayed phase inversion processes, such as lowering the casting temperature or using a soft non-solvent as the coagulation bath, e.g., alcohol.

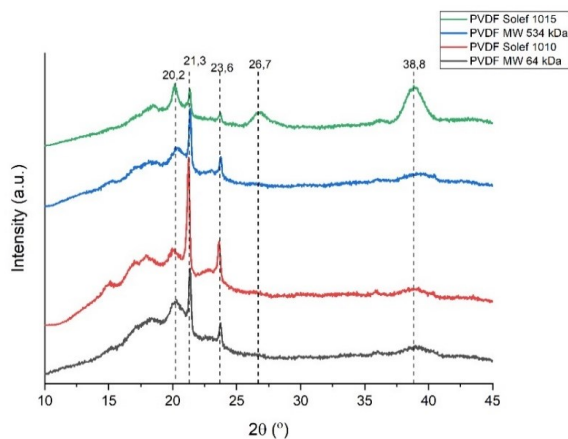


**Figure 3.** XRD diffractogram of PVDF membranes with different molecular weights

**Table 2.** Crystallinity and number of  $\beta$  fractions of each membrane with different molecular weights

PVDF	$\beta$ phase (%)	Crystallinity (%)
PVDF MW 64 kDa	75.11	71.41
PVDF Solef 1010	49.69	69.17
PVDF MW 534 kDa	77.47	86.02
PVDF Solef 1015	41.30	96.50

The difference in molecular weight of PVDF also affects the thermal stability of the produced membrane. Figure 4 and Table 3 represent the TGA thermogram and the degradation temperature ranges of each membrane. The PVDF Solef 1010 membrane has three degradation stages: evaporation from moisture (water vapor) and the breaking of the C–H bond followed by H–F and C=C bonds. The third degradation is caused by the degradation process of the main chain of PVDF [25].

Meanwhile, in PVDF Solef 1015, PVDF MW 64 kDa, and PVDF MW 534 kDa experienced two stages of degradation. Table 3 shows that the membranes with the lowest to highest degradation temperature are PVDF Solef 1010, PVDF MW 534 kDa, PVDF MW 64 kDa, and PVDF Solef 1015. Higher molecular weight tends to have better thermal stability because it has a longer and denser polymer chain, making it more resistant to chemical bond breaking and thermal degradation during heating [29]. Therefore, this research obtained the contrary condition because PVDF MW 64 kDa has higher thermal degradation than PVDF Solef 1010 and PVDF MW 534 kDa.

DSC analysis was performed to determine the effect of PVDF’s molecular weight on the membrane’s melting point. The DSC thermogram is shown in Figure 5, and the melting point of each membrane is shown in Table 4. The lowest to highest melting points are owned by PVDF MW 64 kDa, PVDF MW 534 kDa, PVDF Solef 1015, and PVDF Solef 1010 membranes. The melting point of PVDF Solef 1015 and PVDF MW 534 kDa was lower than Solef 1010. This is because Solef 1010 PVDF membranes have the lowest crystallinity of the other three PVDF membranes, known that the crystallinity of a membrane affects its thermal stability; the higher the crystallinity, the higher the thermal stability [30].

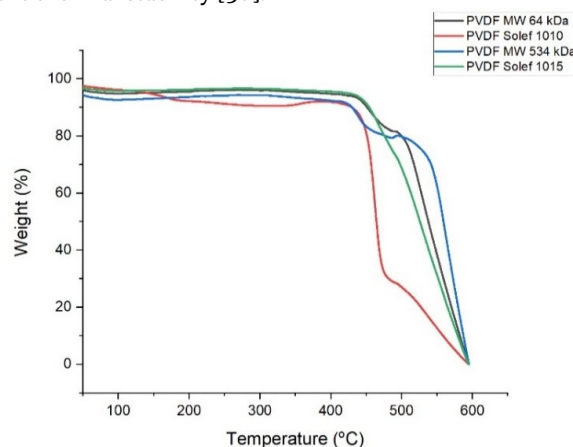


**Figure 4.** TGA thermogram of PVDF membranes with different molecular weights

Table 3. Degradation temperature of each membrane

PVDF	Stage of Degradation					
	I (°C)		II (°C)		III (°C)	
	Onset	Offset	Onset	Offset	Onset	Offset
PVDF MW 64 kDa	421	483	490	600	-	-
PVDF Solef 1010	110	178	410	482	489	600
PVDF MW 534 kDa	415	488	495	600	-	-
PVDF Solef 1015	425	489	490	600	-	-

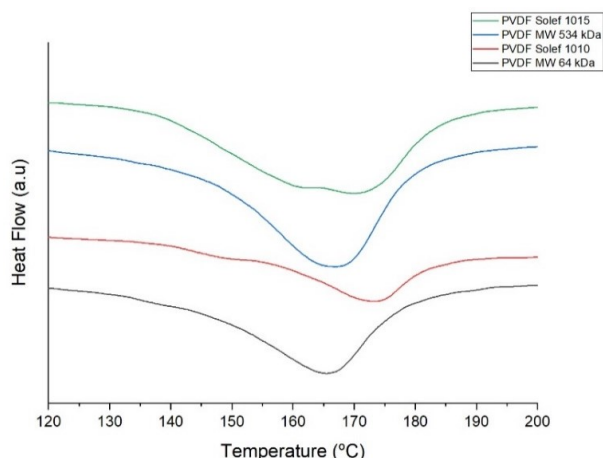


Figure 5. DSC thermogram of PVDF membranes with different molecular weights

In addition, although Solef 1010 has the lowest  $\beta$  phase, it has a higher  $\alpha$  and  $\gamma$  phase; this is in line with data from ATR-FTIR (Figure 2), so Solef 1010 has the highest melting point because  $T_m$   $\alpha$  phase is 167–172°C and  $\gamma$  phase 179–180°C [12]. However, this contradicts findings from prior research [31], indicating that based on the molecular weight of PVDF, an elevation in molecular mass tends to impact the melting point. In this context, a higher molecular weight of the polymer corresponds to an increased melting point.

WCA measurements are performed to determine the effect of molecular weight and temperature on membrane wettability, and the data are presented in Table 5 and Figure 6. In this study, the lowest WCA belongs to PVDF Solef 1010 (55.97°), while PVDF MW 534 kDa has the highest WCA (83°). The study’s results also show a membrane with a molecular weight of 573 kDa (Solef 1015), and using ethanol as a non-solvent produced the roughest membrane surface. The wettability of a membrane can be influenced by its surface roughness, which is influenced by material properties like pore size distribution and molecular weight [32].

A higher molecular weight tends to result in a membrane with a more uneven surface [32], consequently leading to an increased value of the water contact angle (WCA) [10]. Roughness is also influenced by the exchange of solvent-non-solvent by the delay demixing method. It follows the corresponding kinetic rate (rate leading to membrane formation by incorporating PVDF chains into the non-woven support matrix) [10]. A comparison of WCA values from this study with previous studies [10] can be seen in Table 5.

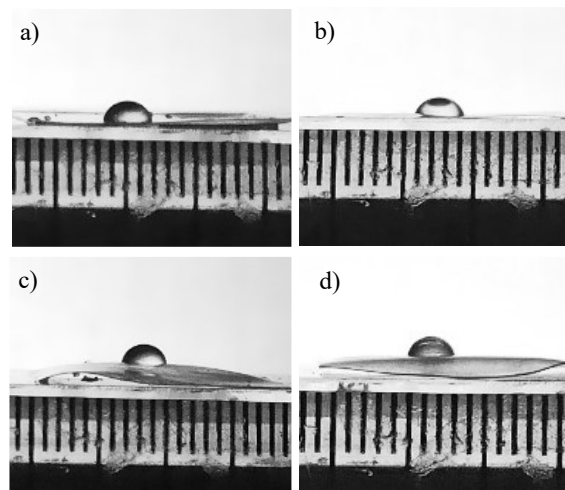


Figure 6. Water contact angle of PVDF membranes: a) MW 64 kDa, b) Solef 1010, c) MW 534 kDa, d) Solef 1015

The molecular weight of PVDF generally affects the physical properties of the prepared membrane. However, in this study, there are some differences with existing research [10, 31, 33]. According to the previous research, the higher the molecular weight of PVDF, the higher the degradation temperature. However, PVDF MW 64 kDa has a higher degradation temperature (421°C) than PVDF Solef 1010 (410°C). In addition, WCA is also affected by membrane roughness and molecular weight, while in PVDF Solef 1010, WCA is lower than PVDF MW 64 kDa, and WCA PVDF Solef 1015 is lower than PVDF MW 534 kDa. PVDF MW 534 kDa has a high  $\beta$  phase and has more potential for use in various fields; however, PVDFs with molecular weight of 64 kDa, 534 kDa, and Solef 1015 have difficulties casting membranes using the immersion precipitation method. Consequently, for the subsequent investigation, PVDF Solef 1010 was used.

Table 4. Melting point of each membrane

PVDF	Molecular Weight (kDa)	Temperature (°C)		
		Onset	Offset	$T_m$
PVDF MW 64 kDa	64	142.5	178.5	165.5
PVDF Solef 1010	352	158.9	182.3	173.0
PVDF MW 534 kDa	534	143.9	180.3	167.0
PVDF Solef 1015	573	137.3	184.4	169.9

Table 5. Comparison of contact angles with previous studies

Molecular weight of PVDF (kDa)	Temperature (°C)	Contact angle (°)	Reference
300–320	60	78	[10]
570–600	60	79	[10]
670–700	60	98	[10]
64	60	74.32	This study
352	60	55.97	This study
534	60	83	This study
585	60	69	This study

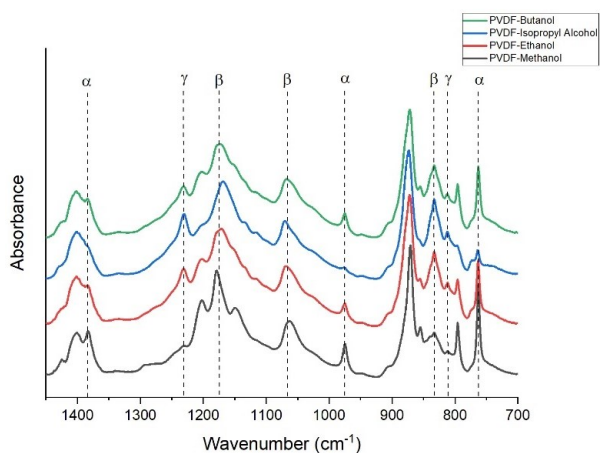


Figure 7. ATR-FTIR spectra of PVDF membranes with different non-solvents

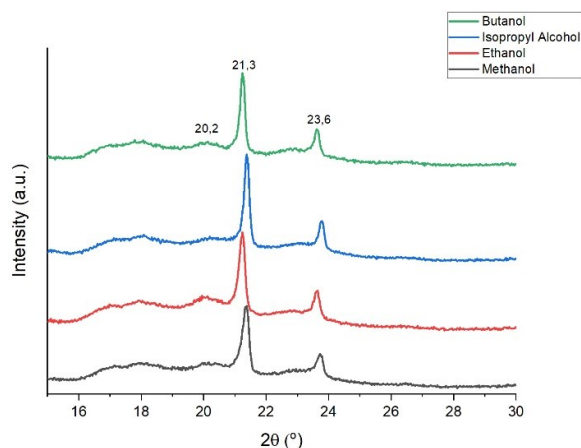


Figure 8. XRD diffractogram of PVDF membranes with different non-solvents

### 3.3. PVDF Membranes with Various Non-Solvents

PVDF Solef 1010 is used in this section because this polymer is the easiest to cast using the immersion precipitation method and produces homogeneous membranes. Non-solvent is one of the essential things in membrane fabrication with this method. The type of non-solvent used for membrane fabrication influences membrane preparation [34]. Different non-solvent alcohols can give other physical properties to the produced membrane. Figure 7 shows the analysis result using ATR-FTIR on PVDF membranes produced from PVDF Solef 1010 with a drying temperature of 60°C for 60 minutes with methanol, ethanol, isopropyl alcohol, and extending to 75 minutes for butanol.

ATR-FTIR spectra show the presence of absorption  $\alpha$  phase at wavenumbers 763, 795, 855, 975, 1148, 1203, 1383, and 1424  $\text{cm}^{-1}$  [12, 26, 27, 35], while the wavenumbers 833  $\text{cm}^{-1}$  can be interpreted as absorption from  $\beta$  phase and  $\gamma$  phase [12, 26, 27]. The XRD data (Figure 8) shows the appearance of the peaks at  $2\theta = 20.24\text{--}20.66^\circ$ , which is the main peak of the  $\beta$  phase [12, 27], at  $2\theta = 21.3^\circ$  and  $23.6^\circ$  are related to polyethylene-like structures [28], then  $2\theta = 17.95^\circ$  and  $25.6^\circ$  indicate diffractogram of the  $\alpha$  phase [12]. Meanwhile, the crystallinity calculation shows the lowest crystallinity belongs to ethanol non-solvent with  $\beta$  phase 49.69%. The crystallinity data and the  $\beta$  phase content of the produced membrane can be seen in Table 6.

The formation of the  $\beta$  phase occurs during the membrane formation process. The  $\beta$  phase and  $\gamma$  phase polymorphs in PVDF membranes have been formed due to certain trans-nucleation of PVDF segments growing in PVDF chain crystal development. This may be due to the interaction between alcohol (non-solvent bath) and PVDF polymers. The O-H functional group present in alcohols has the ability to establish hydrogen bonding interactions with the C-F bonds in polyvinylidene fluoride (PVDF) [36]. It can also be seen in ATR-FTIR spectra that different types of non-solvents can reduce the  $\alpha$  phase and increase the  $\beta$  phase quite well found in isopropyl alcohol spectra.

Membranes produced using ethanol and isopropyl alcohol as non-solvent were analyzed using SEM to determine the cross-section morphology. Morphological analysis using SEM is shown in Figures 9a and 9b. Figure 9a shows that membranes produced using non-solvent ethanol form a finger-like morphology. In Figure 9b, the membrane with non-solvent isopropyl alcohol shows a dense sponge-like morphology. This morphology occurs due to the diffusion of non-solvents and solvents in PVDF membranes. Table 1 shows that the diffusion coefficient in isopropyl alcohol is lower than in ethanol. This indicates that the rate of liquid-liquid phase separation is slower in isopropyl alcohol, resulting in the formation of finger-like macropores being inhibited to some extent, and the structure tends to transform more completely into sponge-like pores. This pore structure has a micron-sized space of many well-connected nanopores [21].

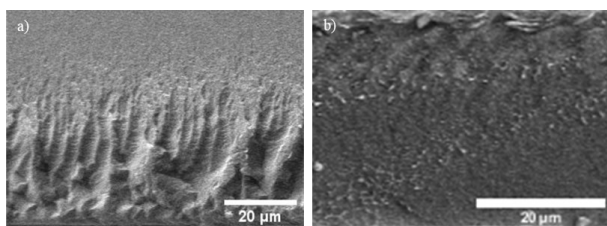


Figure 9. Membrane cross-section morphologies of a) PVDF-ethanol, b) PVDF-isopropyl alcohol

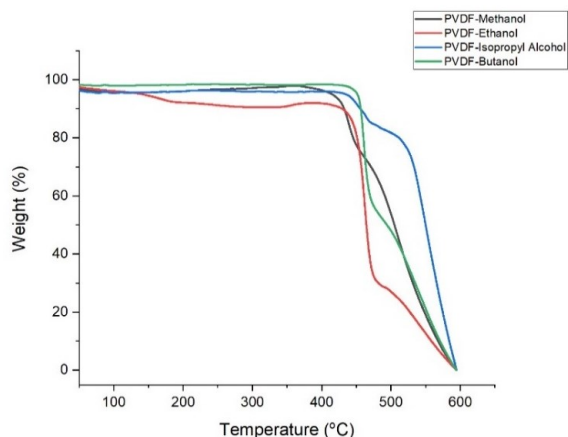


Figure 10. TGA thermogram of PVDF membranes with different non-solvents

The TGA thermogram (Figure 10) shows that different non-solvents also affect the thermal stability of the produced membrane. The three membranes made using methanol, isopropyl alcohol, and butanol undergo two stages of degradation, while the membranes produced using ethanol undergo three stages of degradation. The degradation temperature range of each membrane can be seen in Table 7. Membranes with non-solvent isopropyl alcohol possess the highest degradation temperature. This happens because of the presence of the  $\gamma$  phase, which is a polymorph highly resistant to chemical environments and high temperatures. In comparison, the  $\beta$  phase PVDF is challenging to maintain at high temperatures because the polymer chains of  $\beta$  phase are easily disoriented [12]. This data aligns with ATR-FTIR (Figure 7), where a membrane with non-solvent isopropyl alcohol,  $\gamma$  phase appears reasonably high at wavenumber  $1233\text{ cm}^{-1}$  compared to other non-solvents.

Table 6. Crystallinity and number of  $\beta$  fractions of each membrane with different non-solvents

PVDF Solef 1010-Non solvent	$\beta$ phase (%)	Crystallinity (%)
PVDF Solef 1010-Methanol	27.60	82.43
PVDF Solef 1010-Ethanol	49.69	69.17
PVDF Solef 1010-Isopropyl Alcohol	67.45	81.18
PVDF Solef 1010-Butanol	44.65	78.99

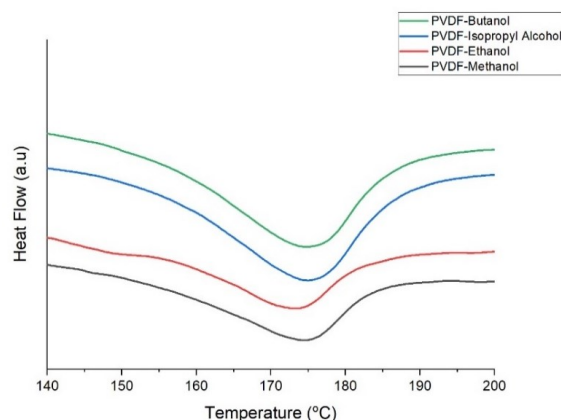


Figure 11. DSC thermogram of PVDF membranes with different non-solvents

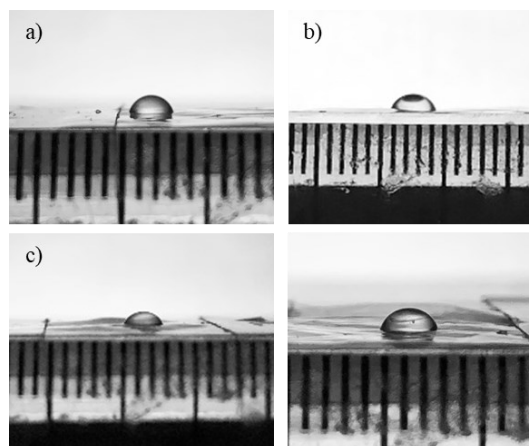


Figure 12. Water contact angle of PVDF membranes with non-solvents: a) methanol, b) ethanol, c) isopropyl alcohol, d) butanol

DSC thermograms and melting point of each PVDF Solef 1010 membrane with some non-solvents are shown in Figure 11 and Table 8. The data show that the non-solvent type in PVDF fabrication has a melting point in the range of  $173\text{--}175^\circ\text{C}$ . Given the proximity of this range, it can be concluded that the difference in non-solvent type does not significantly impact the melting point of the PVDF membrane.

Non-solvents of isopropyl alcohol show the highest wettability, as indicated by the lowest contact angle value. Therefore, this non-solvent is considered most promising for producing PVDF membranes with favorable physical properties [37]. This is also supported by ATR-FTIR results, where isopropyl alcohol non-solvent can increase the  $\beta$ -phase. In addition, TGA analysis also shows that the use of this non-solvent has the best degradation temperature than other non-solvents in PVDF membrane fabrication.

WCA measurements are performed to determine the effect of alcohol on membrane wettability. The results indicate that the produced membrane wettability properties are relatively close. Contact angle values from smallest to largest are  $54.77^\circ$ ,  $55.97^\circ$ ,  $56.03^\circ$ , and  $56.87^\circ$ , corresponding to isopropyl alcohol, ethanol, methanol, and butanol non-solvents, respectively. The images of the water contact angle on the membrane surface are presented in Figure 12a-d.

Table 7. Degradation temperature of each membrane

PVDF Solef 1010–Non solvent	Stage of Degradation					
	I (°C)		II (°C)		III (°C)	
	Onset	Offset	Onset	Offset	Onset	Offset
PVDF Solef 1010–Methanol	369	445	450	600	-	-
PVDF Solef 1010–Ethanol	110	178	410	482	489	600
PVDF Solef 1010–Isopropyl Alcohol	430	468	482	600	-	-
PVDF Solef 1010–Butanol	430	471	481	600	-	-

Table 8. Melting temperature of each membrane

Non-solvent	Temperature (°C)		
	Onset	Offset	T <sub>m</sub>
Methanol	154.7	183.8	174.6
Ethanol	158.9	182.3	173.0
Isopropyl alcohol	143.9	180.3	174.9
Butanol	137.3	184.4	174.8

#### 4. Conclusion

PVDF membrane fabrication with several molecular weight and non-solvent variations has been studied and analyzed. PVDF membranes were prepared using immersion precipitation using several molecular weights of 64 kDa, Solef 1010, 534 kDa, Solef 1015, and several non-solvents. PVDF Solef 1010 has the lowest crystallinity (69.17%) and WCA (55.97°), and it is also the most accessible membrane to cast using the immersion precipitation method compared to the other three PVDFs. Although this membrane's β phase (49.69%) and degradation temperature (410°C) are lower than the other three PVDFs, they can be modified using non-solvents to increase the β phase and degradation temperature. Isopropyl alcohol can increase the β phase of PVDF Solef 1010 to 67.45% and the degradation temperature to 430°C. In addition, PVDF Solef 1010 membrane with non-solvent isopropyl alcohol also has the best surface wettability, indicated by a low WCA of 54.77°.

#### Acknowledgment

The authors are thankful to Lembaga Penelitian dan Pengabdian Masyarakat (LPPM) Universitas Sebelas Maret Surakarta Indonesia for providing financial support through the Fundamental Research Program No. 228/UN27.22/PT.01.03/2023.

#### References

[1] V. F. Cardoso, G. Botelho, S. Lanceros-Méndez, Nonsolvent induced phase separation preparation of poly(vinylidene fluoride)-co-chlorotrifluoroethylene membranes with tailored morphology, piezoelectric phase content and mechanical properties, *Materials & Design*, 88, (2015), 390–397 <https://doi.org/10.1016/j.matdes.2015.09.018>

[2] Edi Pramono, Rifki Alfiansyah, Muhamad Ahdiat, Deana Wahyuningrum, Cynthia Linaya Radiman, Hydrophilic poly(vinylidene fluoride)/bentonite hybrid membranes for microfiltration of dyes,

*Materials Research Express*, 6, 10, (2019), 105376 <https://doi.org/10.1088/2053-1591/ab42e9>

[3] Marco Bolloli, Claire Antonelli, Yannick Molmèret, Fannie Alloin, Cristina Iojoiu, Jean-Yves Sanchez, Nanocomposite poly(vinylidene fluoride) /nanocrystalline cellulose porous membranes as separators for lithium-ion batteries, *Electrochimica Acta*, 214, (2016), 38–48 <https://doi.org/10.1016/j.electacta.2016.08.020>

[4] Dong Zhou, Devaraj Shanmukaraj, Anastasia Tkacheva, Michel Armand, Guoxiu Wang, Polymer Electrolytes for Lithium-Based Batteries: Advances and Prospects, *Chem*, 5, 9, (2019), 2326–2352 <https://doi.org/10.1016/j.chempr.2019.05.009>

[5] Hongrui Xiang, Xiaobo Min, Chong-Jian Tang, Mika Sillanpää, Feiping Zhao, Recent advances in membrane filtration for heavy metal removal from wastewater: A mini review, *Journal of Water Process Engineering*, 49, (2022), 103023 <https://doi.org/10.1016/j.jwpe.2022.103023>

[6] Manojit Pusty, Parasharam M. Shirage, Insights and perspectives on graphene-PVDF based nanocomposite materials for harvesting mechanical energy, *Journal of Alloys and Compounds*, 904, (2022), 164060 <https://doi.org/10.1016/j.jallcom.2022.164060>

[7] Dong Zou, Young Moo Lee, Design strategy of poly(vinylidene fluoride) membranes for water treatment, *Progress in Polymer Science*, 128, (2022), 101535 <https://doi.org/10.1016/j.progpolymsci.2022.101535>

[8] Guo-dong Kang, Yi-ming Cao, Application and modification of poly(vinylidene fluoride) (PVDF) membranes – A review, *Journal of Membrane Science*, 463, (2014), 145–165 <https://doi.org/10.1016/j.memsci.2014.03.055>

[9] Hsu-Hsien Chang, Liang-Kuei Chang, Cheng-Dau Yang, Dar-Jong Lin, Liao-Ping Cheng, Effect of polar rotation on the formation of porous poly(vinylidene fluoride) membranes by immersion precipitation in an alcohol bath, *Journal of Membrane Science*, 513, (2016), 186–196 <https://doi.org/10.1016/j.memsci.2016.04.052>

[10] Monika Haponska, Anna Trojanowska, Adrianna Nogalska, Renata Jastrzab, Tania Gumi, Bartosz Tylkowski, PVDF Membrane Morphology—Influence of Polymer Molecular Weight and Preparation Temperature, *Polymers*, 9, 12, (2017), 718 <https://doi.org/10.3390/polym9120718>

[11] XueMei Tan, Denis Rodrigue, A Review on Porous Polymeric Membrane Preparation. Part II:

- Production Techniques with Polyethylene, Polydimethylsiloxane, Polypropylene, Polyimide, and Polytetrafluoroethylene, *Polymers*, 11, 8, (2019), 1310 <https://doi.org/10.3390/polym11081310>
- [12] Zhaoliang Cui, Naser Tavajohi Hassankiadeh, Yongbing Zhuang, Enrico Drioli, Young Moo Lee, Crystalline polymorphism in poly(vinylidene fluoride) membranes, *Progress in Polymer Science*, 51, (2015), 94–126 <https://doi.org/10.1016/j.progpolymsci.2015.07.007>
- [13] Gregory R. Guillen, Yinjin Pan, Minghua Li, Eric M. V. Hoek, Preparation and Characterization of Membranes Formed by Nonsolvent Induced Phase Separation: A Review, *Industrial & Engineering Chemistry Research*, 50, 7, (2011), 3798–3817 <https://doi.org/10.1021/ie101928r>
- [14] Duc-Trung Tran, Jean-Pierre Méricq, Julie Mendret, Stephan Brosillon, Catherine Faur, Influence of Preparation Temperature on the Properties and Performance of Composite PVDF–TiO<sub>2</sub> Membranes, *Membranes*, 11, 11, (2021), 876 <https://doi.org/10.3390/membranes11110876>
- [15] Zuolong Chen, Dipak Rana, Takeshi Matsuura, Derek Meng, Christopher Q. Lan, Study on structure and vacuum membrane distillation performance of PVDF membranes: II. Influence of molecular weight, *Chemical Engineering Journal*, 276, (2015), 174–184 <https://doi.org/10.1016/j.cej.2015.04.030>
- [16] A. Figoli, S. Simone, A. Criscuoli, S. A. Al-Jilil, F. S. Al Shabouna, H. S. Al-Romaih, E. Di Nicolò, O. A. Al-Harbi, E. Drioli, Hollow fibers for seawater desalination from blends of PVDF with different molecular weights: Morphology, properties and VMD performance, *Polymer*, 55, 6, (2014), 1296–1306 <https://doi.org/10.1016/j.polymer.2014.01.035>
- [17] Naser Tavajohi Hassankiadeh, Zhaoliang Cui, Ji Hoon Kim, Dong Won Shin, Aldo Sanguineti, Vincenzo Arcella, Young Moo Lee, Enrico Drioli, PVDF hollow fiber membranes prepared from green diluent via thermally induced phase separation: Effect of PVDF molecular weight, *Journal of Membrane Science*, 471, (2014), 237–246 <https://doi.org/10.1016/j.memsci.2014.07.060>
- [18] Dan-ying Zuo, Bao-ku Zhu, Jian-hua Cao, You-yi Xu, Influence of Alcohol-Based Nonsolvents on The Formation and Morphology of PVDF Membranes in Phase Inversion Process, *Chinese Journal of Polymer Science*, 24, 03, (2006), 281–289 <https://doi.org/10.1142/S0256767906001308>
- [19] Panu Sukitpaneemit, Tai-Shung Chung, Molecular elucidation of morphology and mechanical properties of PVDF hollow fiber membranes from aspects of phase inversion, crystallization and rheology, *Journal of Membrane Science*, 340, 1, (2009), 192–205 <https://doi.org/10.1016/j.memsci.2009.05.029>
- [20] J. A. van't Hof, A. J. Reuvers, R. M. Boom, H. H. M. Rolevink, C. A. Smolders, Preparation of asymmetric gas separation membranes with high selectivity by a dual-bath coagulation method, *Journal of Membrane Science*, 70, 1, (1992), 17–30 [https://doi.org/10.1016/0376-7388\(92\)80076-V](https://doi.org/10.1016/0376-7388(92)80076-V)
- [21] Arshad Hussain, Andleeb Mehmood, Adil Saleem, Muhammad K. Majeed, Waseem Raza, Rashid Iqbal, Sajid Rauf, Ali Saad, Yonggui Deng, Geng Luo, Kai Zong, Liu Wei, Jun Shen, Dongqing Liu, Xingke Cai, Polyetherimide membrane with tunable porous morphology for safe lithium metal-based batteries, *Chemical Engineering Journal*, 453, (2023), 139804 <https://doi.org/10.1016/j.cej.2022.139804>
- [22] S. Ashtiani, M. Khoshnamvand, P. Číhal, M. Dendisová, A. Randová, D. Bouša, A. Shaliutina-Kolešová, Z. Sofer, K. Friess, Fabrication of a PVDF membrane with tailored morphology and properties via exploring and computing its ternary phase diagram for wastewater treatment and gas separation applications, *RSC Advances*, 10, 66, (2020), 40373–40383 <https://doi.org/10.1039/D0RA07592B>
- [23] Norafiqah Ismail, Mohamed Essalhi, Mahmoud Rahmati, Zhaoliang Cui, Mohamed Khayet, Naser Tavajohi, Experimental and theoretical studies on the formation of pure  $\beta$ -phase polymorphs during fabrication of polyvinylidene fluoride membranes by cyclic carbonate solvents, *Green Chemistry*, 23, 5, (2021), 2130–2147 <https://doi.org/10.1039/D1GC00122A>
- [24] Yang Zhang, Lin Ye, Bopeng Zhang, Yongsheng Chen, Weigao Zhao, Guang Yang, Jie Wang, Hongwei Zhang, Characteristics and performance of PVDF membrane prepared by using NaCl coagulation bath: Relationship between membrane polymorphous structure and organic fouling, *Journal of Membrane Science*, 579, (2019), 22–32 <https://doi.org/10.1016/j.memsci.2019.02.054>
- [25] Masashi Kotobuki, Li Lu, Seruguei V. Savilov, Serguei M. Aldoshin, Poly(vinylidene fluoride)-Based Al Ion Conductive Solid Polymer Electrolyte for Al Battery, *Journal of The Electrochemical Society*, 164, 14, (2017), A3868 <https://doi.org/10.1149/2.1601714jes>
- [26] Xiaomei Cai, Tingping Lei, Daoheng Sun, Liwei Lin, A critical analysis of the  $\alpha$ ,  $\beta$  and  $\gamma$  phases in poly(vinylidene fluoride) using FTIR, *RSC Advances*, 7, 25, (2017), 15382–15389 <https://doi.org/10.1039/C7RA01267E>
- [27] P. Martins, A. C. Lopes, S. Lanceros-Mendez, Electroactive phases of poly(vinylidene fluoride): Determination, processing and applications, *Progress in Polymer Science*, 39, 4, (2014), 683–706 <https://doi.org/10.1016/j.progpolymsci.2013.07.006>
- [28] Hilal Ahmad Rather, Ria Thakore, Ragini Singh, Dhvani Jhala, Sanjay Singh, Rajesh Vasita, Antioxidative study of Cerium Oxide nanoparticle functionalised PCL-Gelatin electrospun fibers for wound healing application, *Bioactive Materials*, 3, 2, (2018), 201–211 <https://doi.org/10.1016/j.bioactmat.2017.09.006>
- [29] Run Tian, Yanxia Zhang, Zhipeng Li, Yangyang Huan, Guangfen Li, Yi Li, Wansheng Li, Coupling effect of PVDF molar mass and carboxyl content in CNTs on microstructure and thermal properties of CNT/PVDF composites, *Materials Research Express*, 5, 6, (2018), 065031 <https://doi.org/10.1088/2053-1591/aac920>
- [30] Jean E. Marshall, Anna Zhenova, Samuel Roberts, Tabitha Petchey, Pengcheng Zhu, Claire E. J. Dancer, Con R. McElroy, Emma Kendrick, Vanessa Goodship, On the Solubility and Stability of Polyvinylidene Fluoride, *Polymers*, 13, 9, (2021), 1354 <https://doi.org/10.3390/polym13091354>

- [31] Zhipeng Hou, Peng Li, Jing Guo, Jiwei Wang, Jianshe Hu, Liqun Yang, The effect of molecular weight on thermal properties and degradation behavior of copolymers based on TMC and DTC, *Polymer Degradation and Stability*, 175, (2020), 109128 <https://doi.org/10.1016/j.polymdegradstab.2020.109128>
- [32] W. Richard Bowen, Teodora A. Doneva, Atomic force microscopy characterization of ultrafiltration membranes: correspondence between surface pore dimensions and molecular weight cut-off, *Surface and Interface Analysis*, 29, 8, (2000), 544-547 [https://doi.org/10.1002/1096-9918\(200008\)29:8<544::AID-SIA901>3.0.CO;2-4](https://doi.org/10.1002/1096-9918(200008)29:8<544::AID-SIA901>3.0.CO;2-4)
- [33] Chen Li, Lei Wang, Xudong Wang, Cuicui Li, Qibin Xu, Guangyuan Li, Fabrication of a SGO/PVDF-g-PSSA composite proton-exchange membrane and its enhanced performance in microbial fuel cells, *Journal of Chemical Technology & Biotechnology*, 94, 2, (2019), 398-408 <https://doi.org/10.1002/jctb.5783>
- [34] M. Bassyouni, M. H. Abdel-Aziz, M. S. Zoromba, S. M. S. Abdel-Hamid, E. Drioli, A review of polymeric nanocomposite membranes for water purification, *J. Ind. Eng. Chem.*, 73, (2019), 19-46 <https://doi.org/10.1016/j.jiec.2019.01.045>
- [35] Junwoo Lee, Sangwoo Lim, Polarization behavior of polyvinylidene fluoride films with the addition of reduced graphene oxide, *J. Ind. Eng. Chem.*, 67, (2018), 478-485 <https://doi.org/10.1016/j.jiec.2018.07.022>
- [36] Guang Hui Teoh, Boon Seng Ooi, Zeinab Abbas Jawad, Siew Chun Low, Impacts of PVDF polymorphism and surface printing micro-roughness on superhydrophobic membrane to desalinate high saline water, *Journal of Environmental Chemical Engineering*, 9, 4, (2021), 105418 <https://doi.org/10.1016/j.jece.2021.105418>
- [37] Mieowkee Chan, Sokchoo Ng, Effect of membrane properties on contact angle, *AIP Conference Proceedings*, 2016, (2018), 020035 <https://doi.org/10.1063/1.5055437>